AD-A098 654 AIR FORCE WEAPONS LAB KIRTLAND AFB NM F/G 20/12
THE EFFECTS OF OXYGEN PRESSURE ON TOTAL DOSE SUSCEPTIBILITY,(U)
JAN 81 R J MAIER
UNCLASSIFIED AFWL-TR-80-106 SBIE-AD-E200 695 NL

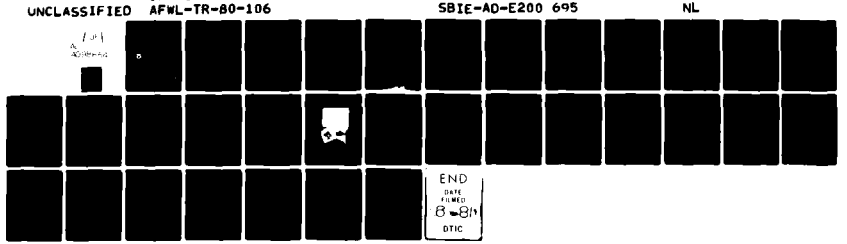

END
DATE FILMED
8-81
DTIC

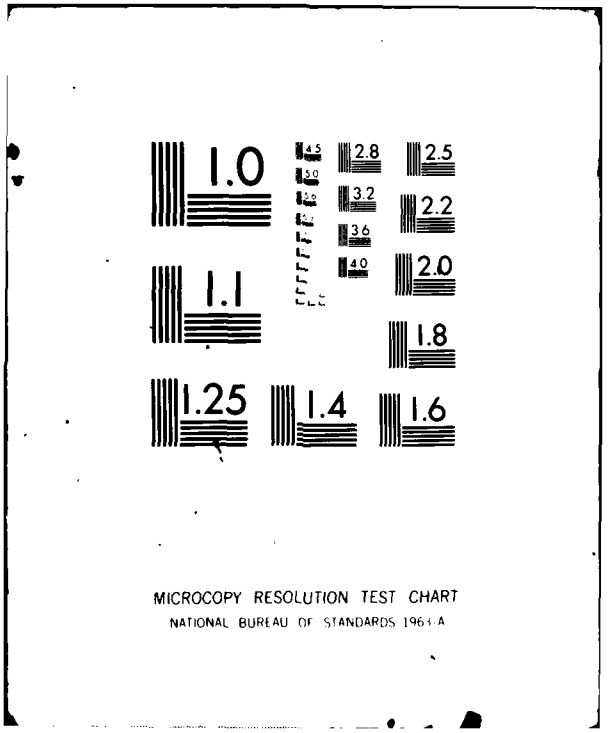
1.0
1.1
1.25
1.4
1.6
1.8
2.0
2.2
2.5
2.8
3.2
3.6
4.0
4.5
5.0
MICROCOPY RESOLUTION TEST CHART
NATIONAL BUREAU OF STANDARDS 1963-A

AFWL-TR-80-106

LEVEL III

AD-E 200 695

AFWL-TR-80-106

AD A098654

THE EFFECTS OF OXYGEN PRESSURE ON TOTAL DOSE SUSCEPTIBILITY

R. J. Maier, Jr.

January 1981

Final Report

AIR FORCE WEAPONS LABORATORY
Air Force Systems Command
Kirtland Air Force Base, NM 87117

AFWL-TR-80-106

This final report was prepared by the Air Force Weapons Laboratory, Kirtland Air Force Base, New Mexico, under Job Order ILIR7805. Mr Roe J. Maier, Jr. (NTYC) was the Laboratory Project Officer-in-Charge.

When US Government drawings, specifications, or other data are used for any purpose other than a definitely related Government procurement operation, the Government thereby incurs no responsibility nor any obligation whatsoever, and the fact that the Government may have formulated, furnished, or in any way supplied the said drawings, specifications, or other data, is not to be regarded by implication or otherwise, as in any manner licensing the holder or any other person or corporation, or conveying any rights or permission to manufacture, use, or sell any patented invention that may in any way be related thereto.

This report has been authored by an employee of the United States Government. Accordingly, the United States Government retains a nonexclusive, royalty-free license to publish or reproduce the material contained herein, or allow others to do so, for the United States Government purposes.

This report has been reviewed by the Public Affairs Office and is releasable to the National Technical Information Service (NTIS). At NTIS, it will be available to the general public, including foreign nations.

This technical report has been reviewed and is approved for publication.

ROE J. MAIER, JR.
Project Officer

CHARLES A. AEBY
Chief, Satellite and C^3 Branch

FOR THE DIRECTOR

NORMAN K. BLOCKER
Colonel, USAF
Chief, Applied Physics Division

DO NOT RETURN THIS COPY. RETAIN OR DESTROY.

UNCLASSIFIED

SECURITY CLASSIFICATION OF THIS PAGE (When Data Entered)

REPORT DOCUMENTATION PAGE		READ INSTRUCTIONS BEFORE COMPLETING FORM
1. REPORT NUMBER AFWL-TR-80-106	2. GOVT ACCESSION NO. AD-A098654	3. RECIPIENT'S CATALOG NUMBER
4. TITLE (and Subtitle) THE EFFECTS OF OXYGEN PRESSURE ON TOTAL DOSE SUSCEPTIBILITY		5. TYPE OF REPORT & PERIOD COVERED Final Report 6. PERFORMING ORG. REPORT NUMBER
7. AUTHOR(s) R. J. Maier, Jr.		8. CONTRACT OR GRANT NUMBER(s)
9. PERFORMING ORGANIZATION NAME AND ADDRESS Air Force Weapons Laboratory (NTYC) Kirtland Air Force Base, NM 87117		10. PROGRAM ELEMENT, PROJECT, TASK AREA & WORK UNIT NUMBERS 61101F/ILIR7805
11. CONTROLLING OFFICE NAME AND ADDRESS Air Force Weapons Laboratory (NTYC) Kirtland Air Force Base, NM 87117		12. REPORT DATE January 1981 13. NUMBER OF PAGES 30
14. MONITORING AGENCY NAME & ADDRESS(if different from Controlling Office)		15. SECURITY CLASS. (of this report) Unclassified 15a. DECLASSIFICATION/DOWNGRADING SCHEDULE

16. DISTRIBUTION STATEMENT (of this Report)

Approved for public release; distribution unlimited.

17. DISTRIBUTION STATEMENT (of the abstract entered in Block 20, if different from Report)

18. SUPPLEMENTARY NOTES

19. KEY WORDS (Continue on reverse side if necessary and identify by block number)

Surface Effects
Total Dose Effects
Si - SiO_2 Interface
Interface States
Interface Fixed Charge
Semiconductor Processing
Oxide Charge

20. ABSTRACT (Continue on reverse side if necessary and identify by block number)

It has been hypothesized that the fixed charge induced by ionizing radiation in the oxide of metal-oxide-silicon (MOS) structures is the result of traps produced by excess silicon. If this is so, then the amount of charging should vary with the oxygen pressure at which the oxide was grown. In this experiment, samples grown at partial pressures of 0.03, 0.04, 0.25, and 1 x 10^5 Pa (atm) and samples grown at 16, 33, 65, 129, 263 and 513 x 10^5 Pa (atm) were exposed to 1 Mrad(Si) Co^{60}. The radiation-induced shifts in voltage, at which the

(Over)

DD FORM 1 JAN 73 1473

UNCLASSIFIED

SECURITY CLASSIFICATION OF THIS PAGE (When Data Entered)

20. ABSTRACT (Continued)

surface potential is at flat band and at midgap, were recorded for an annealing period of 63 days or longer. The results from the partial pressure oxides data supported the hypothesis. An unexpected result was that samples which take longer to grow, anneal faster. This is explained by assuming devitrification.

CONTENTS

INTRODUCTION

A previous article (Ref. 1) predicted that the fixed (surface state) charge (Ref. 3)* produced by ionizing radiation in metal-oxide-silicon (MOS) oxides would vary with the oxidation pressure used to grow the oxides. This susceptibility was measured using partial pressures of oxygen 0.6 through 1 x 10^5 Pa (atms) but a dependence was not seen (Ref. 2). Perhaps the measurements did not cover a wide enough range? To settle this question, another experiment was performed. The results of the experiment were in support of the theory--but also showed that for dry oxides, permanent fixed charge is not the main effect; rather, interface states dominate. The model used in Reference 1 assumes that the susceptibility of the oxide to radiation-induced fixed charge was due to excess silicon centers acting as traps. During oxide growth these centers diffused from the silicon interface through the oxide to the silicon dioxide ambient interface. The model also assumed a uniform density of excess oxygen centers in the oxide, and the density would increase with oxygen partial pressure in the ambient. The model further assumed that excess silicon centers were introduced at a rate proportional to the oxide growth rate and disappeared when either an excess oxygen center or the oxide ambient surface was encountered (ambient interface is totally absorbing or black). This model has been modified and no longer assumes the oxide ambient to be black to excess silicon; it now assumes an excess silicon-oxygen recombination velocity. When the calculation is run with the modified model, it predicts that susceptibility increases with decreasing oxidation pressure.

Such a model requires experimental proof. To perform this experiment, MOS oxides grown on N-doped silicon wafers at partial pressures of 1, 1/4, 1/20, and 1/32 x 10^5 Pa (atms) were prepared by Sandia at 1000°C using argon to dilute the oxygen. These oxides had a target thickness of 40 nm. Also, oxides were prepared by the U.S. Army Electronics and Devices Laboratory (ERADCOM), two samples each at 16, 33, 65, 129, 263 and 513 x 10^5 Pa (atms). These oxides were grown at 900°C in a mild steel pressure vessel and had a target thickness of 200 nm. Preliminary data, taken on the partial pressure

*This term is derived from Reference 3, List of Symbols, "Q_{ss} fixed surface state charge density per unit areas." It is fixed because it is independent of surface potential.

oxides, was obtained from Sandia National Laboratories* and BDM Corporation (Ref. 4). These two sets of data had radically different times at which the after radiation measurements were made and showed that the holes conduction type of annealing (Refs. 5, 6, and 7) was continuing long after irradiation. Thus, a long-term annealing experiment was required.

A preliminary experiment with the ERADCOM samples showed strong annealing past 15 days. The final experiment contains annealing data past 63 days.

Experimentally, it is known that the rapid annealing of fixed charge follows the $(time)^{-\beta}$ form at times after the annealing is 90 percent complete (Refs. 5, 6, and 8). In the analysis, this form, convolved over the irradiation period, is used to separate the permanent fixed charge from the unannealed portion. The resulting values are used to demonstrate the increased permanent fixed charge in partial pressure oxides. Also, it is known that the unannealed portion is proportional to oxide thickness cubed (Refs. 5, 6, and 7). The value of the unannealed portion, divided by thickness cubed, is used to show that oxides which are grown very fast, anneal slowly.

(Throughout this report the new unit, Pascal (Pa), is used. 10^5 Pa equals approximately one atmosphere of pressure. When 10^5 Pa appears, it is followed by (atms) as a reminder.)

*Private communication, W. R. Dawes, Sandia National Laboratories, Jan 78

THEORY

One model (Ref. 1) of the cause of radiation susceptibility due to flat band shift in MOS structures shows that excess silicon centers left near the Si-SiO_2 interface act as traps for holes (Ref. 9). In addition, there is dissolved oxygen in the film (Ref. 3). Defining this dissolved oxygen as an oxygen excess center (Ref. 9), a complete picture of the oxidation process can be drawn, i.e., (1) excess oxygen centers rapidly diffuse throughout the film; (2) at the silicon interface, silicon is injected into the oxide to form excess silicon centers; and, (3) excess silicon centers diffuse toward the oxygen gas interface until they encounter an excess oxygen center or oxygen gas interface and are converted to stoichiometric SiO_2. This model predicts that the number of trapped holes will be growth pressure dependent.

The details of this model can be mathematically expressed by the equations for lossy diffusion.

$$D_{Si} \nabla^2 A_{Si} - \langle\sigma v\rangle A_o A_{Si} = 0 \qquad (1)$$

has

$$A_{Si} = Be^{-\alpha x} + Ce^{\alpha x} \text{ as the one-dimensional solution} \qquad (2)$$

where

$$\alpha = \sqrt{\langle\sigma v\rangle A_o / D_{Si}}$$

D_{Si} is the diffusion constant for excess silicon centers and contains an activation energy $E_{D_{Si}}$.

x is the distance from the Si-SiO_2 interface into the SiO_2.

A_{Si} is the excess silicon center activity (effective silicon center concentration).

$\langle\sigma v\rangle$ is the capture constant of the oxygen excess centers for the silicon excess centers.

A_o is the oxygen excess center activity (effective oxygen center concentration) and is constant if the oxide is growing in the linear region (Ref. 3).

B and C are constants to be determined by boundary conditions.

The boundary conditions are:

a. At x = o, the Si-SiO_2 interface, the flux of centers, as determined by Fick's equation, must equal the rate that Si excess centers enter the oxide, i.e.,

$$J_{Si} = (-D_{Si}\nabla A_{Si})_{x=o} = D_{Si}\alpha(Be^{-\alpha x} - Ce^{+\alpha x}) \tag{3}$$

$$K\alpha = J_{Si}/D_{Si}\alpha = B\text{-}C \tag{4}$$

J_{Si} is proportional to A_o, i.e., α^2; thus K is constant with respect to α.

b. At x = t (t = the thickness of the oxide), the presence of the oxygen atmosphere produces a velocity of excess silicon centers toward the interface. This velocity is analogous to the surface recombination velocity in semiductors.

$$J_{Si} = -D_{Si}\nabla A_{Si} = UA_{Si} \tag{5}$$

or

$$L(Be^{-\alpha t} + Ce^{\alpha t}) = Be^{-\alpha t} - Ce^{\alpha t} \tag{6}$$

where

U is the surface velocity and U is proportional to A_o and thus proportional to α^2.

$L = U/D_{Si}\alpha$ is proportioned to α

$= H\alpha$

With the above boundary conditions, the solution for A_{Si} is

$$A_{Si} = K \frac{(1+L)e^{\alpha(t-x)} + (1-L)e^{-\alpha(t-x)}}{(1+L)e^{\alpha t} - (1-L)e^{-\alpha t}} \tag{7}$$

The distribution of hole traps is not experimentally measurable. The charge induced at the silicon interface and the charge centroid have been measured (Ref. 10). These are found by integrating Equation 7.

These two integrals are

$$Q = \int_0^t \frac{t-x}{t} A_{Si} dx$$

$$= K \frac{(1+L)\left[e^{\alpha(t-x_o)}\left(t-x_o-\frac{1}{\alpha}\right)+\frac{1}{\alpha}\right] - (1-L)\left[e^{-\alpha(t-x_o)}\left(t-x_o+\frac{1}{\alpha}\right)-\frac{1}{\alpha}\right]}{(1+L)e^{\alpha t} - (1-L)e^{-\alpha t}} \tag{8}$$

$$\bar{X} = \int_0^t x A_{Si} dx \Big/ \int_0^t A_{Si} dx$$

$$= \frac{(1+L)\left[e^{\alpha(t-x_o)}\left(x_o+\frac{1}{\alpha}\right) - \left(t+\frac{1}{\alpha}\right)\right] - (1-L)\left[e^{-\alpha(t-x_o)}\left(x_o-\frac{1}{\alpha}\right) - \left(t-\frac{1}{\alpha}\right)\right]}{(1+L)e^{\alpha t} - (1-L)e^{-\alpha t}} \tag{9}$$

Where x_o is the distance into the oxide beyond which holes cannot tunnel from trap to silicon interface.

In Figure 1a-d, the values of Q/K parametric in α are plotted. Each figure has a different value of H. No further change occurs for values of H larger than that of Figure 1a or smaller than that of Figure 1d. The $\bar{X}$s shown are for t = 100 nm. Reference 10 states that the upper limit of $\bar{X}$ for a 100 nm, 1000°C, dry oxide is 5 nm. This is useful for determining which curve is the curve for the 1 x 10^5 Pa (atm) sample. That curve is the one for α^{-1} = 1.25 nm, or 2.5 nm; 16 x 10^5 Pa (atm) should be α = 0.16 - 0.32

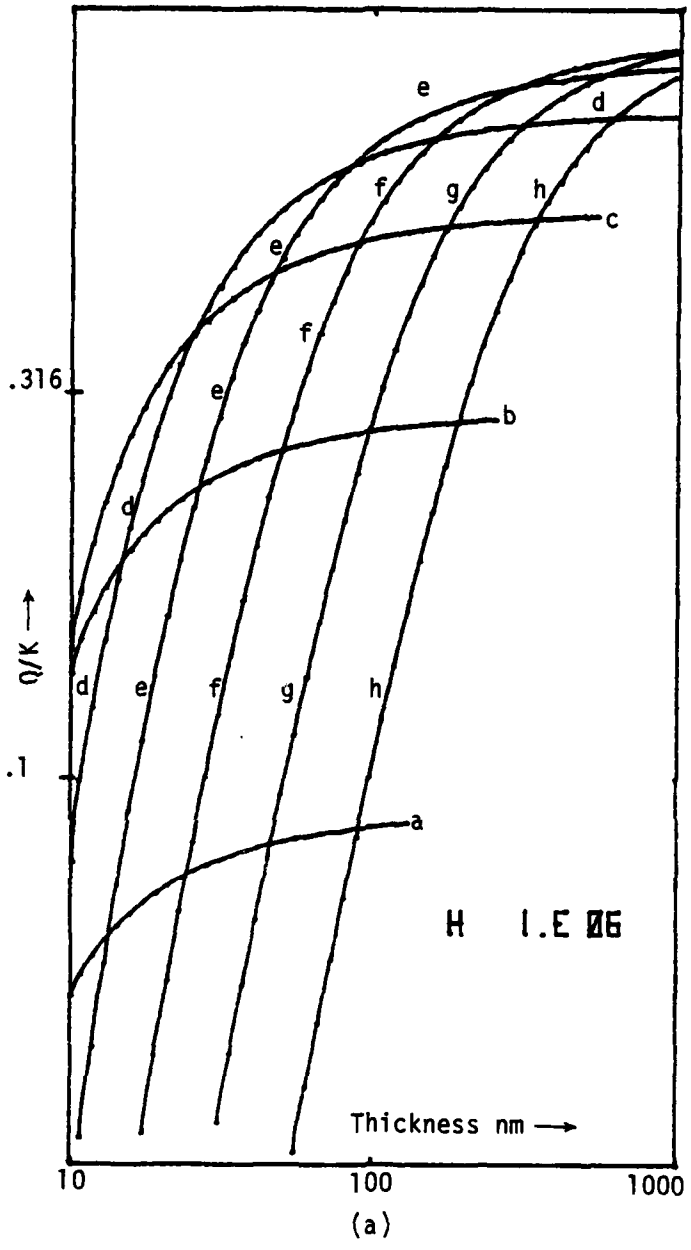

Figure 1. Values of Q/K vs thickness.

(Value of Q/K vs thickness for α^{-1} = a. 1.25; b. 2.5; c. 5; d. 10; e. 20; f. 40; g. 80; h. 160 nm. The values for $\bar{x}$ are a. 3.75; b. 5; c. 7.5; d. 12.49 nm; x_g = 2.5 nm.)

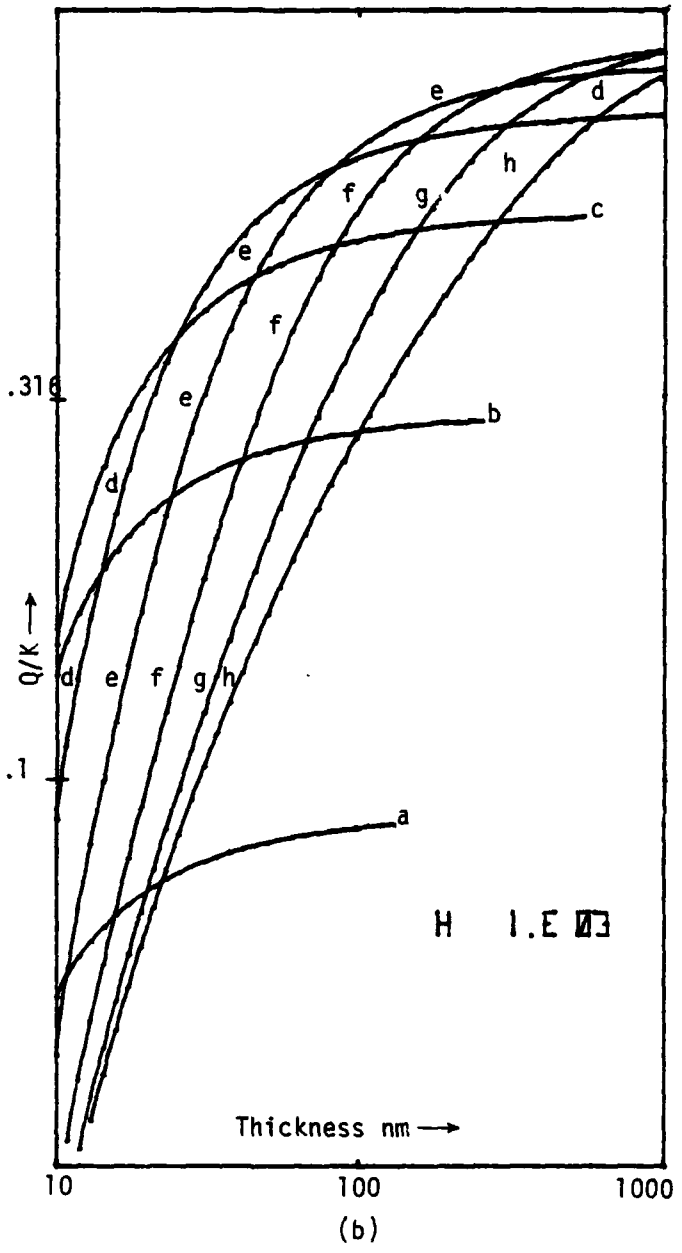

(b)

Figure 1. Continued.

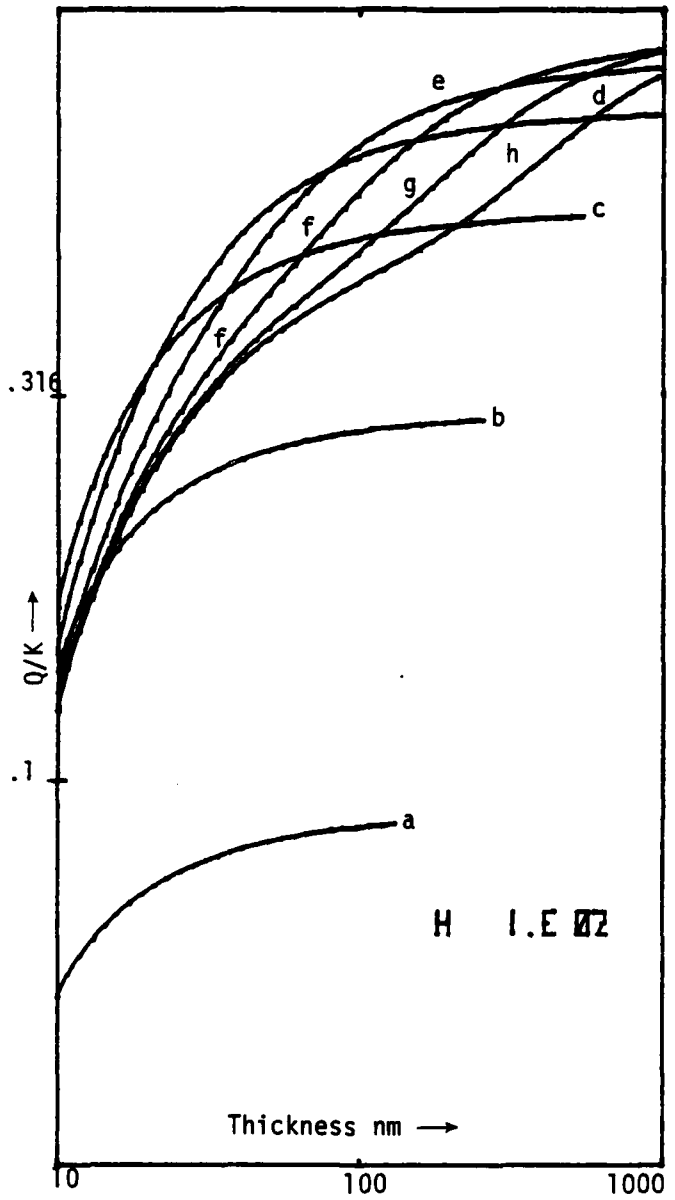

(c)

Figure 1. Continued.

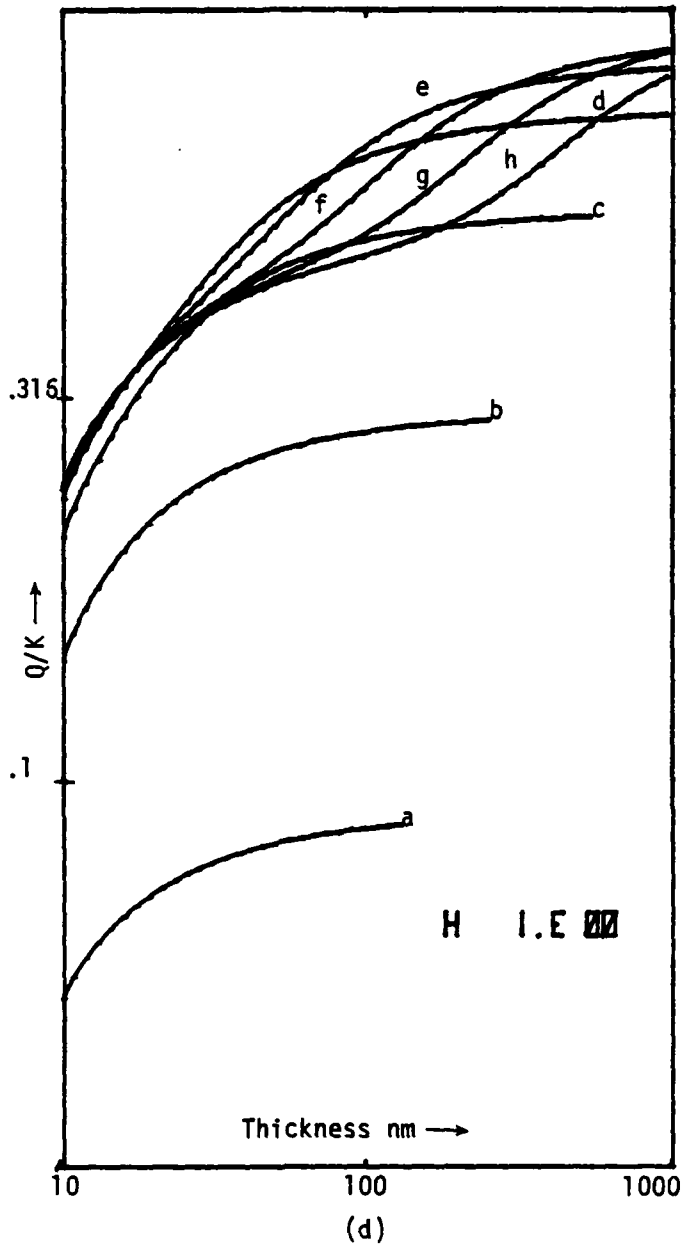

Figure 1. Concluded.

(not shown). The 3×10^3 Pa (atm) sample should have $\alpha = 72 - 144$. Note that the curves e - h which are affected by the value of H are not for reasonable pressures.

EXPERIMENTAL APPARATUS AND PROCEDURES

The following describes the test sample, the capacitance voltage measuring methods, and the preliminary experiments. The preliminary experiments showed the need for an annealing experiment and what could be done to make the resulting data more useful.

Experimental Test Devices

Special oxides were prepared by Sandia and ERADCOM for this experiment. The Sandia oxides were grown on N-type wafers doped with about 10^{16} donors per cm^3 at 1000°C in argon-oxygen ambients of 0/1, 7.5/2.5, 9.5/0.5, and 9.7/0.3. The aluminum dot electrodes were evaporated through a shadow mask and sintered. Prior to oxidation, the wafers were cleaned; a field oxide 15 min dry, 90 min steam at 1100°C was grown; and, the field oxide was stripped in buffered HF. ERADCOM prepared two wafers by growing a field oxide as above and cutting the wafers into samples approximately 8.5 by 25.4 mm. One sample from each wafer was placed in a mild steel vertical reactor. The field oxide was stripped just prior to loading the reactor. During oxidation the bottom of the reactor was 900°C. Due to a temperature gradient, the top of the reactor was cooler than the bottom. Ellipsometry was used at about 6.4 and 12.7 mm from the bottom of the sample to determine thickness. The characteristics of the samples are listed in Table 1. Note, the rate of thickness change in the ERADCOM samples with distance from the bottom is not the same for all samples.

TABLE 1. PRESSURE, THICKNESS AND GROWTH TIME

Pressure x 10^5 Pa	Oxide Thickness (nm) Bottom	Center	Growth Time (min)	A
513.0	192.3	192.3	16	0.23
263.0	211.8	207.4	26	0.31
129.0	214.7	209.9	43	0.38
65.0	193.3	189.8	70	0.42
33.0	184.6	182.4	114	0.49
16.0	185.5	182.2	187	0.61
1.0	42.3		60	7.05
0.25	51.4		240	8.57
0.04	57.6		1200	12.00
0.03	61.1		1920	10.29

The quantity A is the thickness divided by both pressure and growth time. This is done to show that growth rate is not strictly proportional to pressure; if it were, A would be constant.

Apparatus

The experiment required a measurement which was primarily dependent on fixed charge. The usual measures of total dose susceptibility, the change in flat-band or threshold voltage, contain large shifts due to the charge in the interface states. It is accepted that the interface states in the upper half of the band gap are generally acceptors, and that the states in the lower half are donors. Thus, when the Fermi level is in the center of the band gap, the charge in the interface states should be minimal. For this experiment, it is assumed that the change in midgap voltage (ΔV_{mg}) is the measure of the fixed charge accumulation (Ref. 11). To measure V_{mg}, C-V curves were taken using an HP4271A LCR Meter, which uses 1 MHz input. The space charge capacitances for flat-band and midgap were computed from a preirradiation curve, and the voltages at which these capacitances occurred were obtained from the preirradiation and postirradiation curves. The difference in the midgap voltage and the flat-band voltages taken before and after irradiation was calculated. The C-V curves were taken under the control of an HP9820 calculator with plotter. To conserve time, the calculator was programmed to use the 4271 LCR Meter to search for the correct capacitance and determine the voltage at which that capacitance occurred.

During exposure the samples were clamped in the aluminum holder shown in Figure 2. Contact to the capacitor dot was made through the aluminum foil. The aluminum foil was pressed against the sample by .635cm foam, and nylon screws were used to hold the aluminum plates together. These holders did not produce reliable contracts, and later it was found that some electrodes had been floating during exposure. The floating devices were easily detected and the data can be treated as exposures biased at zero field.

Preliminary Data

Sandia processed four wafers at each partial pressure and then performed irradiations on one complete set. In Table 2, the change in midgap voltage is shown. BDM also irradiated a set to verify a hardness assurance screen.

Figure 2. Samples and sample holders. (Holders were used to bias samples during exposures.)

TABLE 2. ΔV_{mg} FOR PARTIAL PRESSURE OXIDE

Sample	ΔV_{mg} Sandia	ΔV_{mg} BDM	Correction Factor	Calculation
1	-1.52	-0.30	1.000	1.22
1/4	-2.12	-0.52	0.686	1.32
1/20	-4.00	-0.95	0.504	2.16
1/32	-3.95	-1.59	0.455	1.59

The observed ΔV_{mg} were actually larger than given above, but since each oxide had a different thickness, the values were reduced by the correction factor $(423/\text{thickness})^2$. A significant difference exists between the Sandia and BDM data; however, Sandia makes their measurements shortly after irradiation while BDM waited 24 hrs. Clearly, the less susceptible oxides are annealing more. The column labeled calculation was obtained by subtracting the BDM data from the Sandia data and multiplying by (423/thickness). With the exception of the 1/20 x 10^5 Pa (atm) sample, the pressure dependence is greatly reduced. The calculation would correspond to the unannealed portion in the Sandia data. These data made apparent the requirement for measurements taken after annealing was complete.

One sample each grown at 513, 263, 129 and 16 x 10^5 Pa (atm) were irradiated to 10^6 rads in 105.75 minutes at the AFWL 5-kCi Co^{60} source. One set of C-V curves was taken soon (1 hr) after irradiation. Successive sets were taken after 1, 3, 7, 15, 31 and 63 days.

From the first set, the need for more data, taken the first day was obvious. Because taking C-V curves was very time comsuming, a much faster search program was written. This program measured V_{mg} and V_{FB} only. Data were taken 0.125, 0.25, 0.5, 1, 2, 4, 8, 16, 32, and 64 days after the start of irradiation.

It was not possible to control temperature during annealing well enough to allow comparison of the rates of annealing from different samples. Though this comparison was not the object of the experiment, it was nevertheless desirable. This problem was solved only by working with the samples in pairs, with each pair kept together and thereby subject to the same temperature

history. The pairs used were identified by their growth pressures in units of x 10^5 Pa (atm) (1, 0.25); (0.04, 0.03); (16, 65); (513, 33) and (263, 129). The annealing rates of samples grown at different pressures can be compared only between members of the same pair.

DATA AND DATA ANALYSIS

After the methods were developed, the final set of data was taken. To be assured of getting adequate data, measurements were made on 16 capacitor dots on each sample. In Figure 3, the partial pressure pairs data are shown. In Figure 4, the high-pressure-samples data are shown.

Note, in Figure 3, the clear separation into two modes. It is assumed that the wrinkles in the aluminum foil shown in Figure 2 prevented contact and the devices with less shift were not biased. In Figure 3, the greater radiation susceptibility of devices grown at lower pressure is apparent. In Figure 4, the most pronounced difference is the larger early $-\Delta V_{mg}$ values in the higher pressure sample, in each pair.

The individual annealing curves were not smooth. Also, it was generally not possible to prove that certain points on the curve were bad and could be disregarded. As a result, good fits to annealing theory were not obtained.

Annealing theory (Refs. 1 and 5) predicts that annealing of a voltage shift from a pulse of radiation follows the form

$$\Delta V = V_\infty + A'/T^\beta \tag{10}$$

where T is time and β, V_∞ and A' are constants.

For Co^{60} exposures, which are steady state, it is necessary to convolve this, i.e.,

$$\Delta V = V_\infty + \frac{A}{T_e}\int_0^{T_e} \frac{dT'}{(T-T')^\beta}$$

$$= V_\infty + \frac{A}{T}\left[T^{1-\beta} - (T-T_e)^{1-\beta}\right] \tag{11}$$

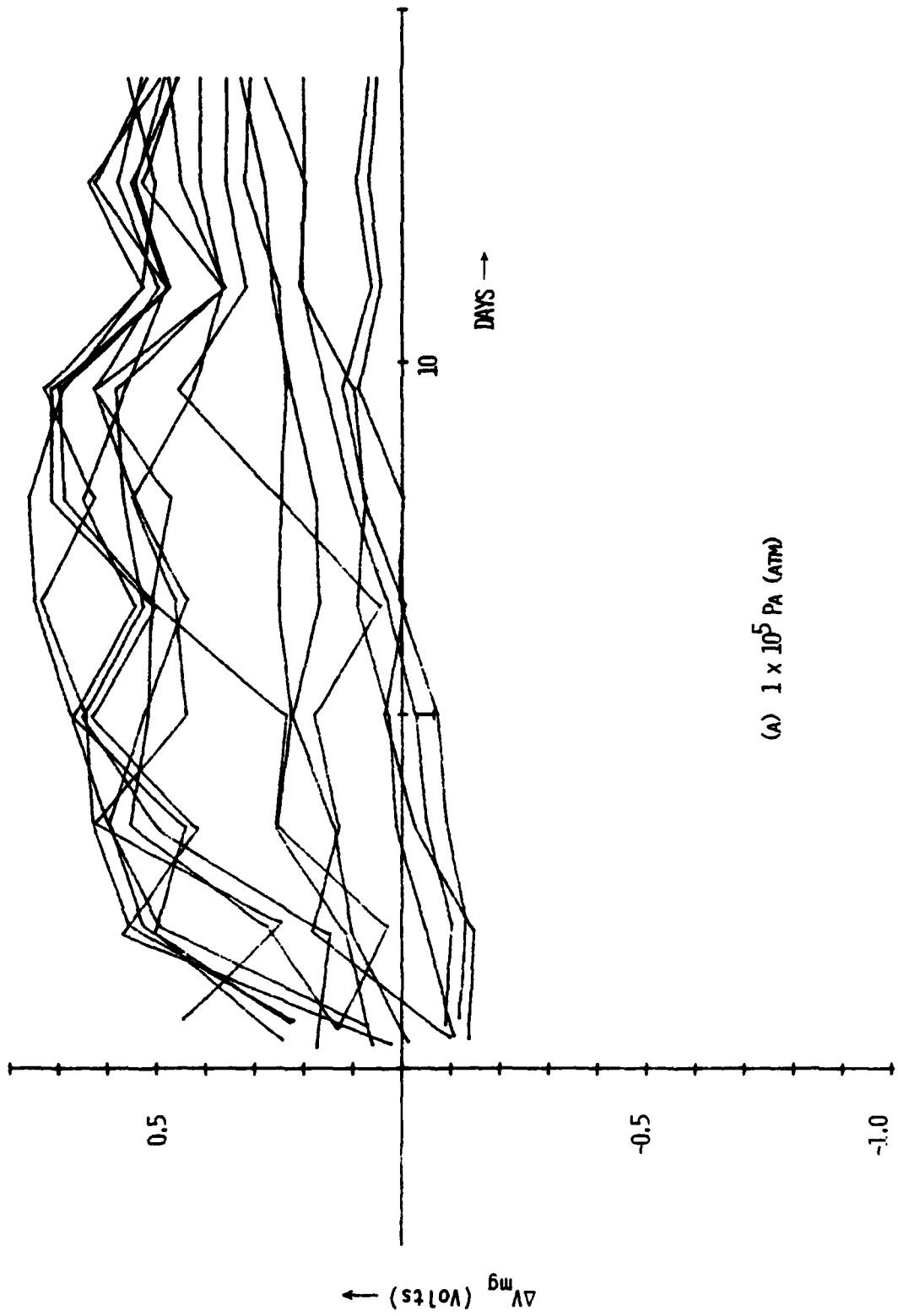

Figure 3. Annealing curves of the partial pressure samples. (Note the different scales for voltage.)

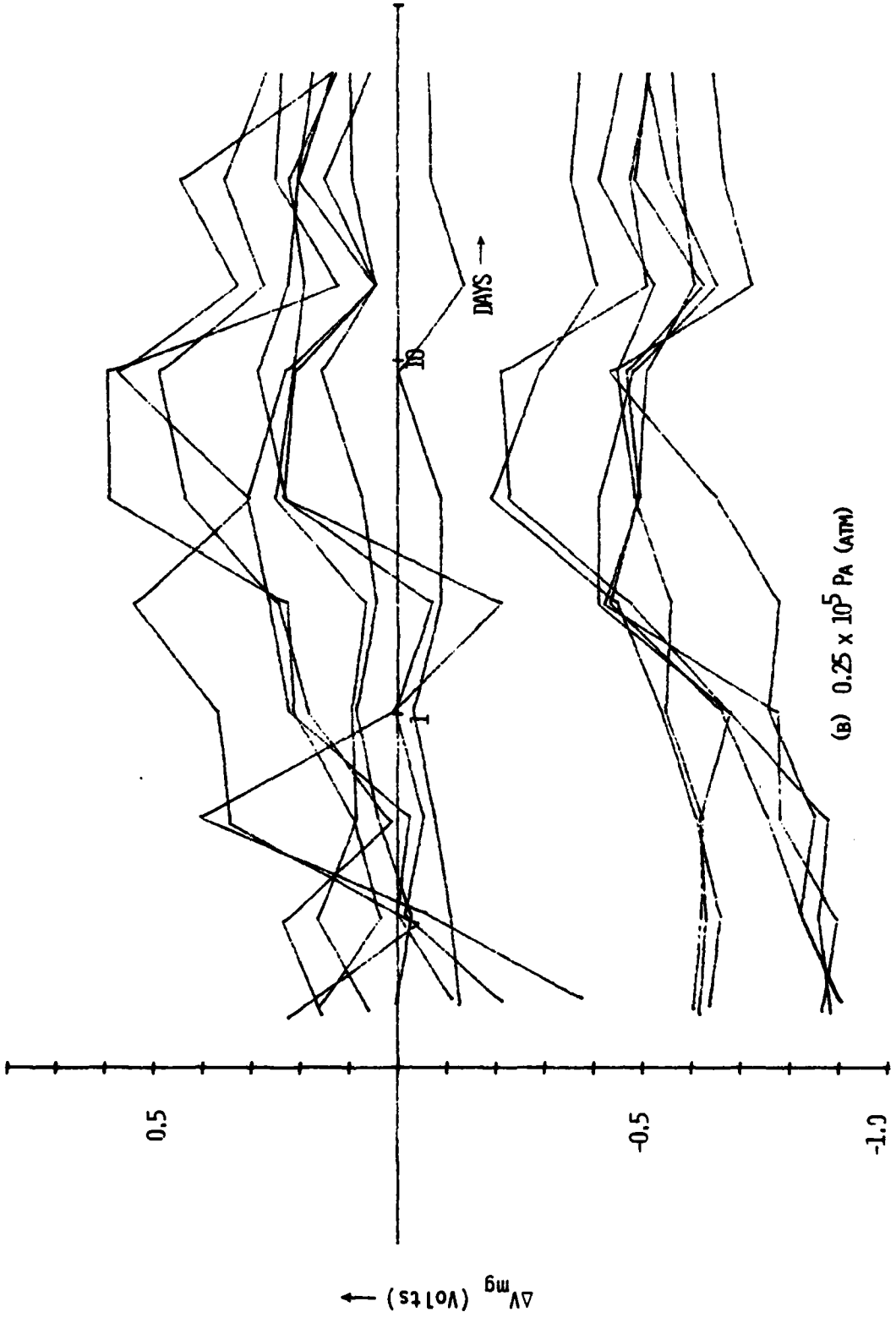

(B) 0.25×10^5 Pa (ATM)

Figure 3. Continued.

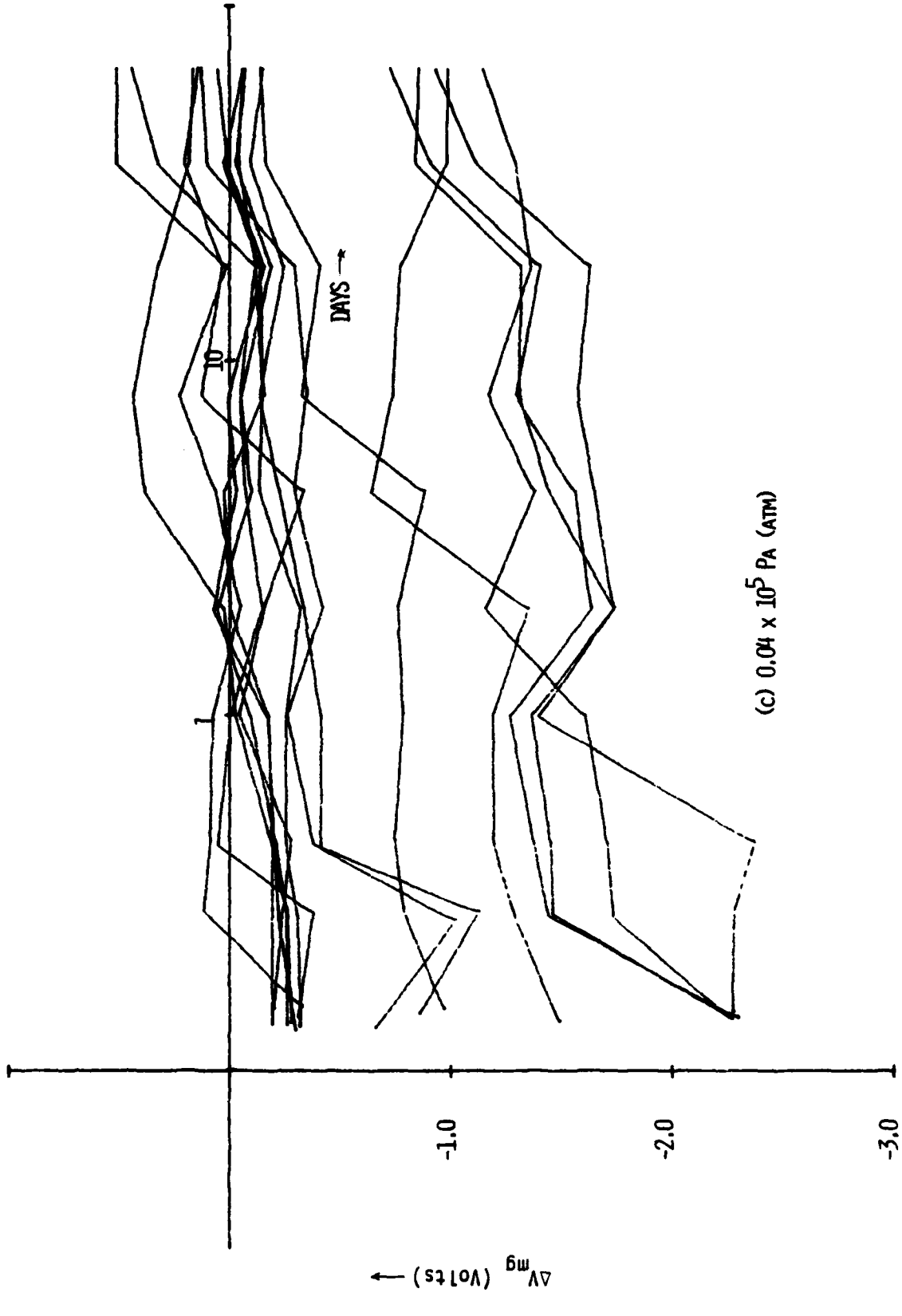

(c) 0.04×10^5 PA (ATM)

Figure 3. Continued.

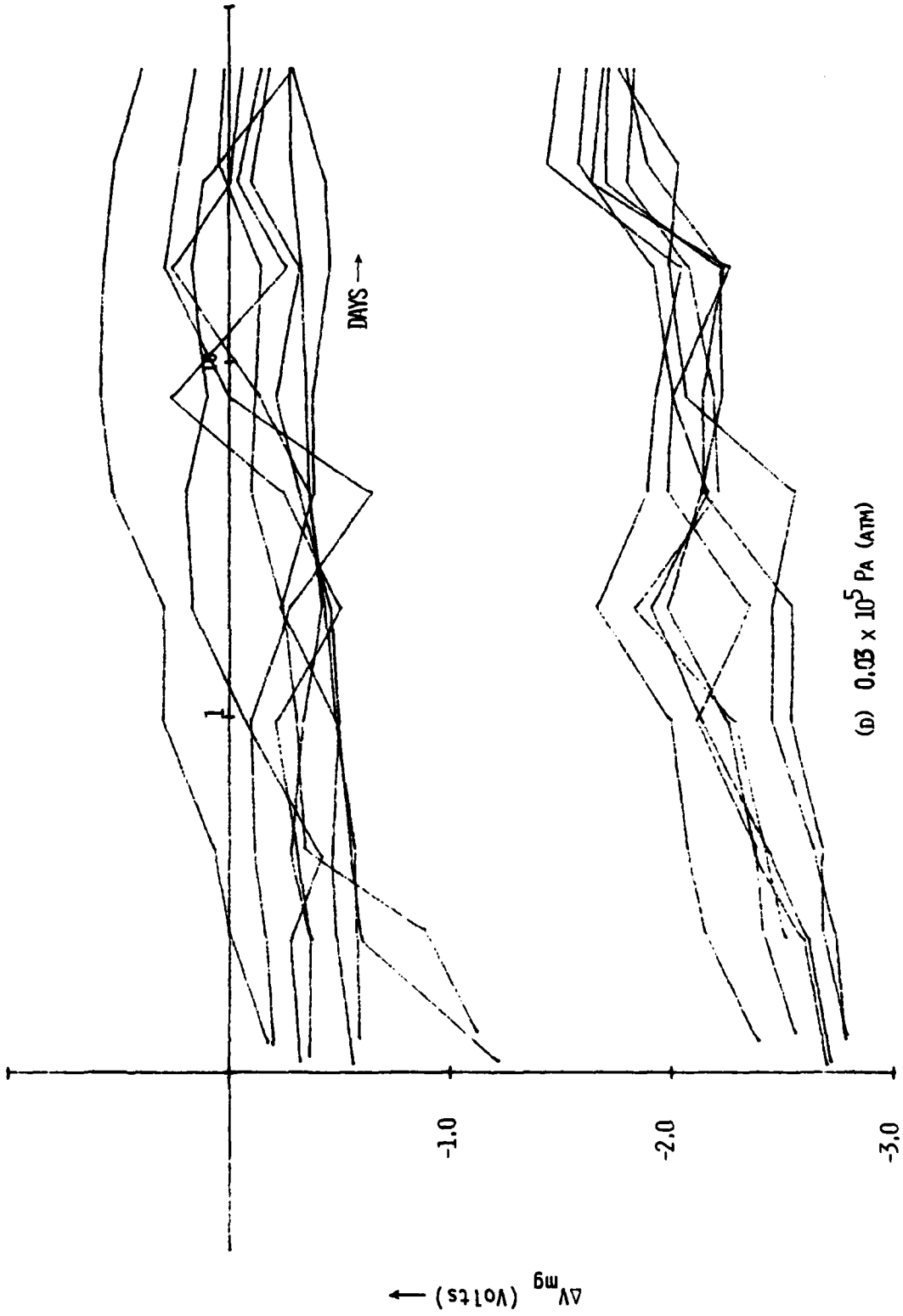

(b) 0.03×10^5 Pa (atm)

Figure 3. Concluded.

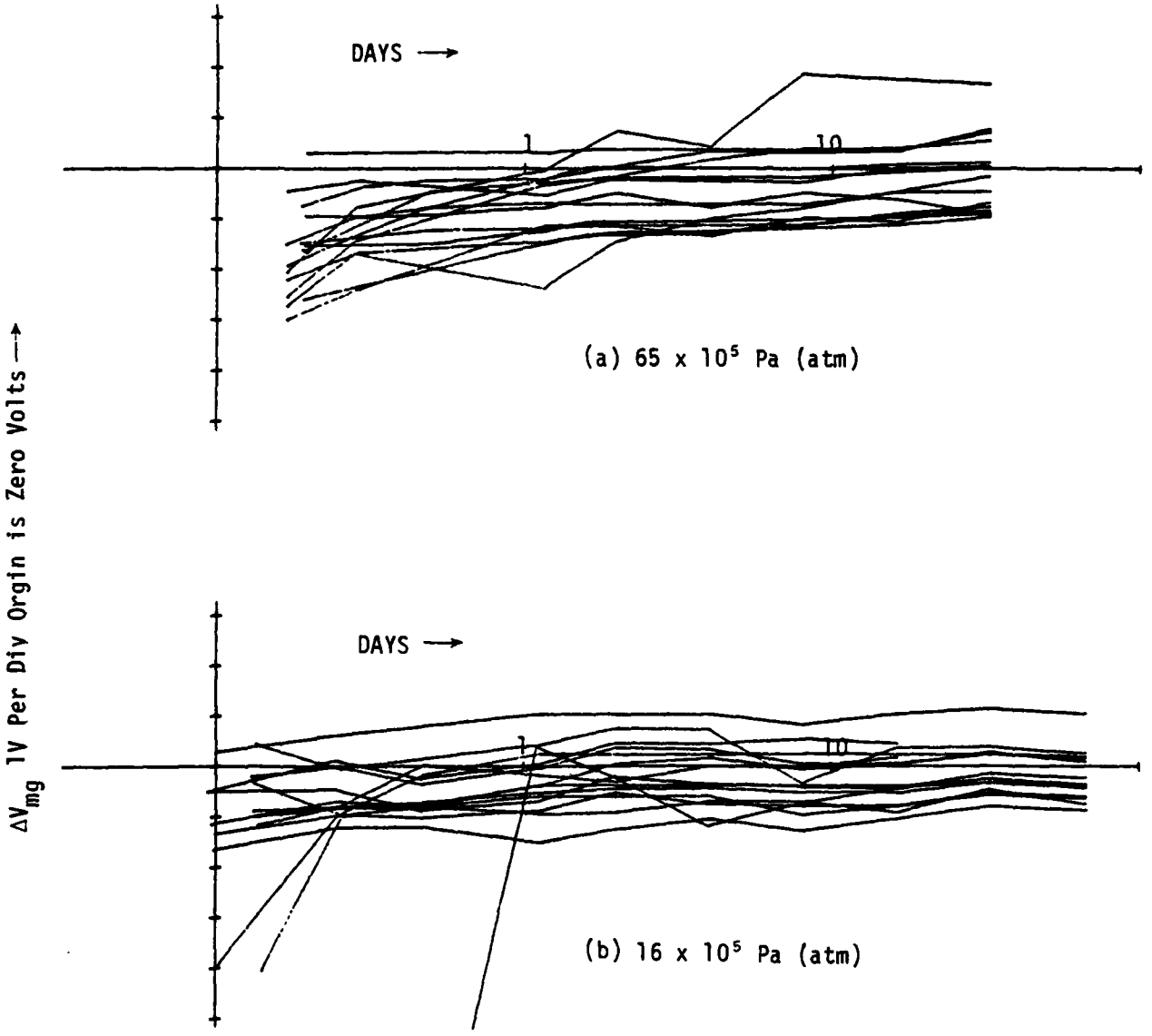

Figure 4. Annealing curves from the high pressure samples. (Vertical comparisons cannot be made because of the different temperature histories.)

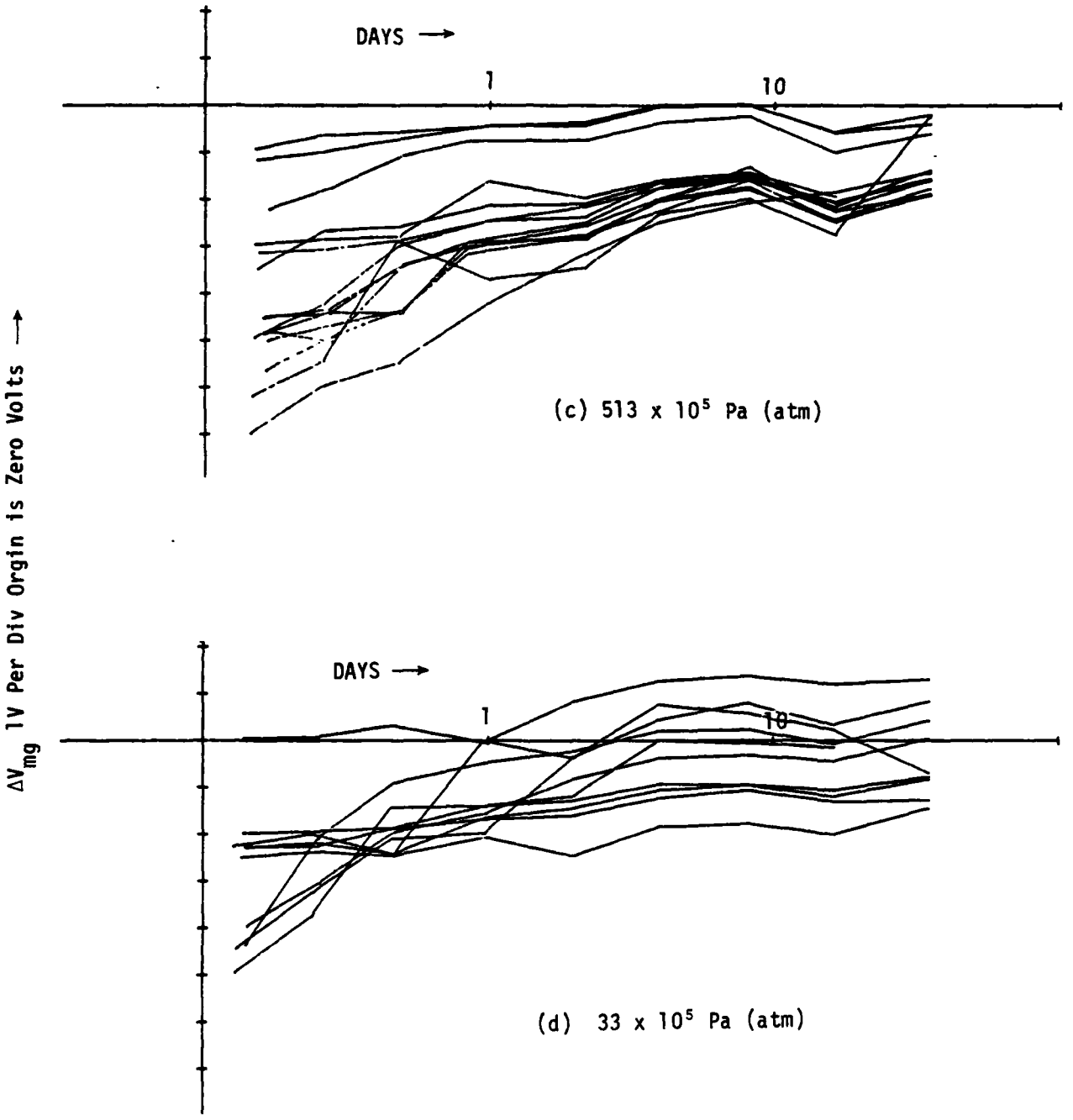

Figure 4. Continued.

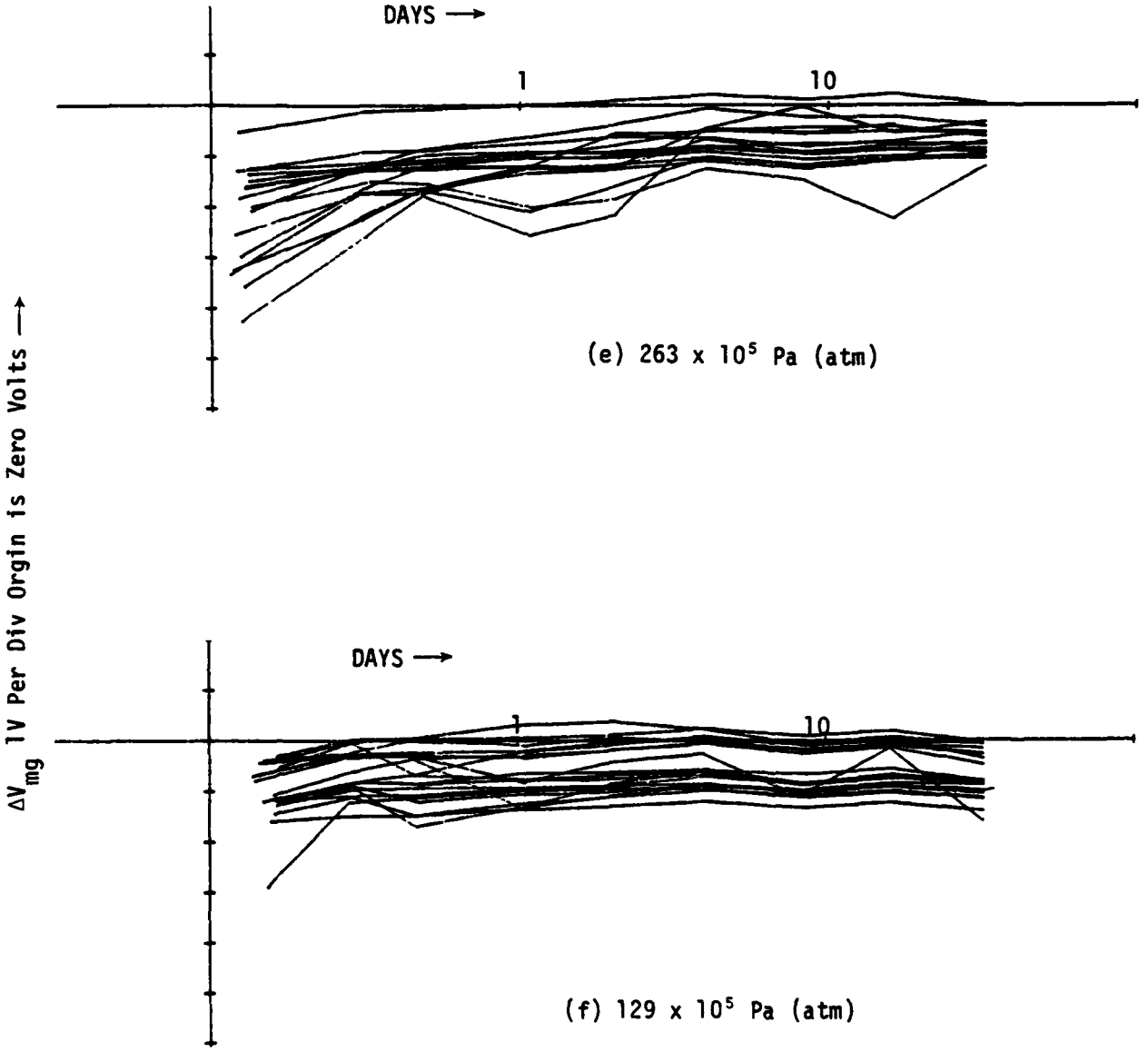

Figure 4. Concluded.

where

V_∞ is the permanent voltage shift and is proportional to thickness squared

β is a constant for each annealing curve and is between 0-1

$A = A'/(1-\beta)$ is a constant and is proportional to thickness cubed

T_e is the exposure time

This form was least square fitted to each annealing curve to obtain values for V_∞, A and β. Widely varying values of β were obtained. A small β such as 0.1 would correspond to annealing out to thousands of days and would result in too small a value for V_∞. Thus, the least squares fit was applied to smooth the curve, and the Values ΔV_{mg} at 0.5 and 50 days were calculated from the fit. The value of ΔV_{mg} at 50 days was subtracted from the value at 0.5 day and the difference was treated as the unannealed portion at 0.5 day. This difference was multiplied by (100 nm/thickness)^3 to correct for oxide thickness variations (Refs. 5, 6 and 7). In this case, the oxide thickness was found from the measurement of oxide capacitance for each individual capacitor. The value at 50 days was treated as the permanent value and was multiplied by (100 nm/thickness)^2 to correct for thickness.* For the partial pressure oxides, the data were separated into the two modes (0.25 MV/cm, floating), and averages were taken for permanent and unannealed fractions. These are listed in Table 3 along with the standard deviation $S^2 = \Sigma(V_i - \overline{V})^2/(n-1)$. The error listed with the mean is the error of the mean $S/\sqrt{n}$.

*If the oxide is thicker proportionally, more holes are created and drift to the Si-SiO_2 interface to be trapped; and since the surface charge creates an electric field, the thicker oxide needs proportionally more voltage to counter the surface charge, thus the thickness squared correction.

TABLE 3. VOLTAGE SHIFTS: V_{mg} PERMANENT AND UNANNEALED PORTIONS FOR THE PARTIAL PRESSURE OXIDES

For 0.25 MV/cm Bias

	Pressure x 10^5 Pa	ΔV Permanent	S_{per}	ΔV Unannealed	S_{un}
PAIR	1	1.05 ± 0.16	0.43	-1.65 ± 0.21	0.37
	0.25	-1.58 ± 0.12	0.34	-1.14 ± 0.09	0.25
PAIR	0.04	-2.64 ± 0.24	0.54	-2.124 ± 0.6	1.37
	0.03	-3.89 ± 0.11	0.30	-2.052 ± 0.18	0.47

For Floating Bias

PAIR	1	2.87 ± 0.11	0.34	-1.5 ± 0.31	0.93
	0.25	0.70 ± 0.16	0.47	-0.72 ± 0.12	0.38
PAIR	0.04	0.08 ± 0.13	0.44	-1.22 ± 0.20	0.68
	0.03	-0.068 ± 0.18	0.55	-0.899 ± 0.09	0.26

The values for permanent voltage shift are clearly more positive for the higher pressure. Note the large positive shifts for the 1 x 10^5 Pa (atm) sample. This means that interface states are contributing as much shift as permanent fixed charge. This prevents a quantitative comparison with theory. Because of the temperature history, the comparisons of the unannealed fraction must be done in pairs. Note that the higher pressure member of the pair has a greater unannealed fraction.

Because of the temperature gradient during the oxidation of the pressure oxides, comparisons can be made only between capacitor electrodes formed on that part of the sample that was near the bottom of the reactor. In Table 4 these data are listed. Position 1 is the bottom position, Position 2 is the next one up, and Position 3 is the third one up. In all cases except Position 3 (513, 33), the unannealed fraction is larger for the higher pressure member of the pair. For the permanent damage, the opposite is generally true. Lastly, note how small the values in Table 4 are compared to the values in Table 3. This is because of the (100 nm/thickness)^2 and (100 nm/thickness)^3 corrections. However, these corrections must be made if the two oxides are to be compared, i.e., there is less charge in the pressure oxides.

TABLE 4. VOLTAGE SHIFTS: PERMANENT AND UNANNEALED FOR THE PRESSURE OXIDES

atm	Position 1		Position 2		Position 3	
	Unannealed	Permanent	Unannealed	Permanent	Unannealed	Permanent
16	-0.055	-0.038	-0.034	-0.077	-0.044	-0.067
65			-0.641	-0.12	-0.14	-0.18
33	-0.15	0.076	-0.27	0.048	-0.38	0.28
513	-0.42	-0.25	-0.29	-0.33	-0.28	-0.34
129	-0.011	-0.18	-0.018	-0.033	-0.006	-0.15
263	-0.12	-0.046	-0.094	-0.061	-0.036	-0.23

CONCLUSIONS

This experiment resulted in data which support the following:

a. Permanent fixed charge induced by ionizing radiation is greater for SiO_2 films on Si which are grown at reduced pressure and less for films grown at increased pressure.

b. The rate of conduction of holes out of these films can be increased by reducing oxide growth rate by reducing growth pressure.

c. The model which describes the permanent fixed charge as holes trapped on excess silicon centers.

d. The model which describes the conduction of the last few percent of the holes from the oxide as slowed by trapping sites produced by wide fluctuations of the Si-O-Si bond angle (Ref. 12).

The author wishes to thank Dr. W. R. Dawes at Sandia and Dr. R. J. Zeto at ERADCOM for preparation of the MOS oxide samples.

REFERENCES

1. Maier, R. J., "Silicon Lattice Constraints on Structure of Interface States," IEEE Trans. on Muc. Sci., Vol NS-22, p. 1558, Dec 76.

2. Derbenwick, G. F., and Gregory, B. L., "Process Optimization of Radiation Hardened CMOS Integrated Circuits," IEEE Trans. on Nuc. Sci., Vol NS-22, No. 6, p. 2151, Dec 75.

3. Grove, S. A., "Physics and Technology of Semiconductor Devices," John Wiley and Sons, Inc., 1967.

4. Young, P. A., Total Ionizing Dose Screens Program, AFWL-TR-80-130, Air Force Weapons Laboratory, Kirtland Air Force Base, N. Mex., to be published.

5. McLean, F. B., and Ausman, G. A., "Simple Approximate Solutions to Continuance Time Random Walk Transport," Phys Rev B-15, No. 2, p. 1052, Jan 77.

6. Boesch, H. E., McLean, F. B., McGarrity, J. M. and Winokur, P., "Enhanced Flatband Voltage Recovery in Hardened Thin MOS Capacitors," IEEE Trans. on Nuc. Sci., Vol NS-25, No. 6, p. 1237, Dec 78.

7. Sander, H. H. and Gregory, B. L., "Unified Model of Damage Annealing in CMOS, From Freeze-In to Transient Annealing," IEEE Trans. on Nuc. Sci., Vol NS-22, No. 6, Dec 75.

8. Maier, R. J., "A Model for the Discharge of Radiation-Induced Space Charge in MOSFET's," presented at the IEEE Annual Conference on Nuclear and Space Radiation Effects, Seattle WA, Jul 72.

9. Deal, B. E., Sklar, M., Grove, A. S., and Snow, E. H., "Characteristics of the Surface State Charge (Q_{SS}) of Thermally Oxidized Silicon," J. Electro-Chem Soc., Vol 114, No. 3, p. 266, 1967.

10. DiMaria, D. J., Weinberg, Z. A., and Aitken, J. M., "Location of Positive Charges in SiO_2 Films on Si Generated by VUV Photons, X-rays and High Field Stressing," J. Appl. Phys., Vol 48, No. 3, Mar 77.

11. Lee, H. S., "Metal-Oxide-Semiconductor Instability Produced by Electron-Beam Evaporation of Aluminum Gates," IEEE Trans on Elec Dev, Vol ED-25, No. 7, Jul 78.

12. Hughes, R. C. and Emin, D., "Small Polaron Formation and Motion of Holes in a - SiO_2," The Physics of SiO_2 and its Interfaces, p. 14, New York: Pergamon Press, 1978.

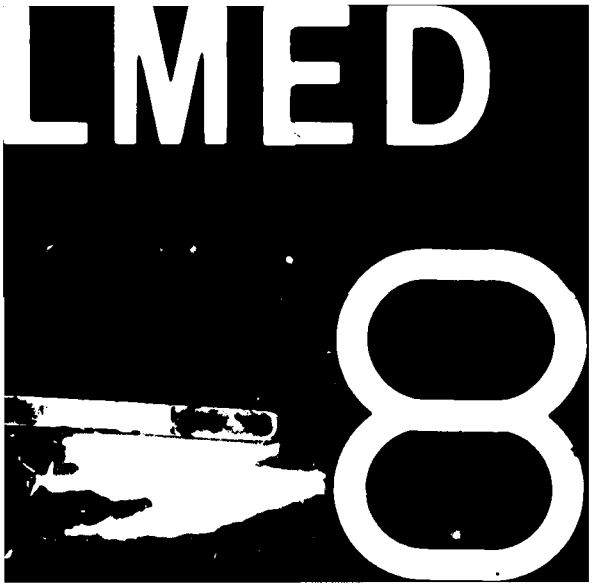
LMED
8